European Journal of Medicinal Chemistry 146 (2018) 206–219

Contents lists available at ScienceDirect

European Journal of Medicinal Chemistry

journal homepage: http://www.elsevier.com/locate/ejmech

Research paper

Design, synthesis and biological evaluation of novel indole-benzimidazole hybrids targeting estrogen receptor alpha (ER-α)

Ramit Singla [a], Kunj Bihari Gupta [b], Shishir Upadhyay [c], Monisha Dhiman [b], Vikas Jaitak [a, *]

[a] Centre for Pharmaceutical Sciences and Natural Products, Central University of Punjab, Bathinda, India
[b] Centre for Biochemistry and Microbial Sciences, Central University of Punjab, Bathinda, India
[c] Centre for Animal Sciences, Central University of Punjab, Bathinda, India

ARTICLE INFO

Article history:
Received 11 August 2017
Received in revised form
15 January 2018
Accepted 16 January 2018

Keywords:
Breast cancer
Estrogen receptor alpha
Induced fit
Indole-benzimidazole hybrids
RT-PCR
Western blotting

ABSTRACT

In the course of efforts to develop novel selective estrogen receptor modulators (SERMs), indole-benzimidazole hybrids were designed and synthesised by fusing the indole nucleus with benzimidazole. All the compounds were first inspected for anti-proliferative activity using ER-α responsive T47D breast cancer cell lines and ER-α binding assay. From this study, two representative bromo substituted compounds **5f** and **8f** were found to be most active and thus were escalated for gene expression studies for targeting ER-α. Cell imaging experiment clearly suggest that compounds were able to cross cell membrane and accumulate thus causing cytotoxicity. RT-PCR and Western blotting experiments further supported that both compounds altered the expression of mRNA and receptor protein of ER-α, thereby preventing the further transactivation and signalling pathway in T47D cells lines. Structural investigation from induced fit simulation study suggest that compound **5f** and **8f** bind in antagonistic conformation similar to bazedoxifene by extensive hydrogen bonding and Van der Waals forces. All these results strongly indicate that compound **5f** and **8f** represents a novel potent ER-α antagonist properties and will proved promising in the discovery of SERM for the management of breast cancer.

© 2018 Elsevier Masson SAS. All rights reserved.

1. Introduction

Breast cancer (BC) is the most common malignancy and deadly cancer which occupies second place after lung cancer, in the list of cancers with the highest mortality rates among women [1]. Hormonal therapy is the first line treatment used in the treatment of estrogen-sensitive BC. As the majority of BC is primarily estrogen-dependent, and its propensity of incidence is approximately 55% in pre-menopausal women and 75% in post-menopausal women. This therapy efficiently blocks the stimulating effect of estrogen in BC [2]. At least 70% of BC patients are categorized as having estrogen receptor (ER) positive cancer because growth of the tumour cells occurs by ER-α activation [3]. In response to estrogen binding, ER-α dimerizes, binds to estrogen response element (ERE) of DNA, and undergoes a conformational change in the ligand binding domain which further facilitates the recruitment of coactivators [4,5]. In addition to genomic signalling, it is accepted that ER-α has non-genomic signalling functions, which correlate with multidrug resistance [6]. In the case of BC, this non-genomic signalling can involve full length receptor or other isoform as well as cross talks with other growth factor receptor or cytoplasmic kinases such as Src [7].

Selective Estrogen Receptor Modulators (SERMs) are chemical entities which reduces the action of estrogen by binding to ER (ERα or ERβ subtypes) in cells [8]. Tamoxifen is a first generation of SERM which significantly reduces the incidence of BC. Although, tamoxifen served as a benchmark in the treatment of BC, but its usage was limited due to stimulatory effects on endometrial cells, increased the risk of development and progression of endometrial cancer and resistance [4,9]. Second generation SERM were developed for reducing the incidence of uterine cancer associated with usage of tamoxifen have also reported side effects like instigates hot flashes, intensified risk of blood clots, deep vein thrombosis and pulmonary embolism. In view of toxicity and adverse effects associated with these drugs bazedoxifene a third-generation SERM was introduced for the treatment of BC and osteoporosis [4,10]. Bazedoxifene was developed combining the essential pharmacophoric features of raloxifene, by substituting the benzothiophene core of raloxifene by indole [11]. Bazedoxifene binds to both ER-α and ER-β, but with a

* Corresponding author.
E-mail address: vikas.jaitak@cup.edu.in (V. Jaitak).

https://doi.org/10.1016/j.ejmech.2018.01.051
0223-5234/© 2018 Elsevier Masson SAS. All rights reserved.

slightly higher affinity for ER-α. It has been reported that the inhibitory effect of bazedoxifene is associated with ER-α down-regulation and cell cycle arrest [4]. Recently, bazedoxifene in combination with palbociclib have been used for treatment of metastatic BC at stage IV [12,13].

One of the main objectives of medicinal chemistry from its very inception has been the search for new compounds that exhibit novel physical, chemical and biological properties. Combination of structural features of two or more functionally active substances into one molecule may lead to synergism, enhancement or modulation of the desired characteristics of individual components. Another tempting feature of this approach is molecular hybrids which can also address the problem of incidence of drug resistance [14]. As single molecule containing more than one pharmacophore, each with different mode of action, could be beneficial for the treatment of cancer and can reduce the chances of drug resistance [15–17]. Recently isatin-quinazoline hybrids have been synthesized and have shown promising antiproliferative activity against liver HepG2, breast MCF-7, and colon HT-29 cancer cell lines [18].

It has been reported that 2-arylindole derivative are selective towards the ER-α and antagonize the action of oestradiol in BC cells and uterus tissues [19]. Further, benzimidazole derivatives have been developed for targeting ER-α by diminishing ERE response in a dose dependent manner [10]. Taking these structural features in account, in the present study we have designed and synthesised new synthetic indole-benzimdazole hybrids as putative SERM for targeting ER-α for the management of hormone dependent BC (HDBC). The synthesised molecules were characterised by NMR, IR and HRMS. Compounds were analysed for the anticancer activity using ER-α expressing T47D cell lines, ER-α binding assay, semi-quantitative RT-PCR, western blotting and confocal microscopy. Molecular docking was used to identify, the possible binding modes of indole-benzimdazole hybrids with ER-α.

2. Results and discussion

2.1. Design and synthesis of indole-benzimidazole derivatives

Indole based compounds have a tremendous potential for the development of chemotherapeutic agents. By the virtue of structural analysis, it has been found that 1-benzyl-indole-3-carbinol, which is an analog of indole-3-carbinol (I3C) was found to be thousand times more potent in comparison to indole-3-carbinol in suppression of both estrogen dependent and independent BC cell lines [20]. 2-arylindole derivative have shown one hundred thirty times fold selectivity towards the ER-α (human ER-α/β IC_{50} 2/259 nM) and antagonize the action of estradiol in MCF-7 (IC_{50} 30 nM) cancer cells and uterus tissues [19]. ERA923 is an indole derivative anti-estrogenic compound, equally effective as tamoxifen and overcome the resistance associated with tamoxifen, tested *in-vitro* and *in-vivo* [21]. Recent developments on 2-substituted benzimidazoles have revealed that varied heterocycles at 2-position yielded potent anticancer agents at various carcinoma cell lines [22–24]. It has been observed that majority of classical SERMs approved for targeting BC contains OH or F [25] functionalisation. In our designed compounds we have applied the concept of monovalent bioisosteres. In medicinal chemistry, bioisosteres are chemical substituents or groups with similar physical or chemical properties which produce broadly similar biological properties to another chemical compound. In the present hybrids the NH serves as a monovalent bioisosteres for the OH [26], which serves the purpose of OH in SERMs for interaction with the essential amino acids residues present in the active site of ER-α. The striking feature of the derivatives having potential anticancer activity is aromatic substitution at 2-position of benzimidazole [27] and free amino group of benzimidazole moiety acts as hydrogen bond donor in the receptor cavity of target ER-α [28]. Therefore, we proposed that *N*-benzylated indole-benzimidazole hybrids (**5**) and N-H indole-benzimidazole hybrids (**8**), pharmacophore designed on the basis of structural feature of indole and benzimidazole derivatives may act as a potential antiproliferative agents targeting BC (Fig. 1).

The *N*-benzylated indole-benzimidazole hybrids (**5a-j**) and N-H indole-benzimidazole hybrids (**8**) were synthesised by the general route with high to moderate yields as described in Scheme 1 and Scheme 2 respectively. The N-position of the starting material ethyl indole-2-carboxylate (**1**) was benzylated using benzyl bromide in the presence of potassium hydroxide using DMSO as polar aprotic solvent to give ethyl-1-benzyl-1H-indole-2-carboxylate (**2**). Compound **2** was reduced to (1-benzyl-1H-indol-2-yl)methanol **(3)** in presence of $LiAlH_4$ under dry THF conditions. Compound **3** was oxidised to 1-benzyl-1H-indole-2-carbaldehyde **(4)** by using activated manganese dioxide in dry CH_2Cl_2. For the synthesis of *N*-benzylated indole-benzimidazole hybrids (**5**), the intermolecular cyclisation of **4** with corresponding diamine in presence of TEA yielded ten compounds (**5a-j).** It should be noted that compounds **5a-j** hitherto unknown in chemical literature and were purified using flash chromatography and unambiguously characterised spectroscopically using ^1H, ^{13}C- NMR, IR and HRMS.

N-H indole-benzimidazole derivatives (**8a-k**) were synthesised from starting material ethyl indole-2-carboxylate (**1**), which was reduced to (1H-indol-2-yl) methanol (**6**) in presence of $LiAlH_4$ and dry THF. Compound **6** was oxidised to 1H-indole-2-carbaldehyde (**7**), by using activated manganese dioxide and dry CH_2Cl_2. For the synthesis of N-H indole-benzimidazole derivatives (**8**), the intermolecular cyclisation of **7** with corresponding diamine in presence of TEA yielded the target eleven N-H indole-benzimidazole derivatives (**8a-k)**. The synthesised derivatives were analysed by ^1H, ^{13}C- NMR, IR and HRMS.

2.2. Biological evaluation of indole-benzimidazole derivatives

HDBC is primarily due to the overexpression of ER- α and diminishing activity of ER-β. The T47D cell lines is a BC cell line, which shows dominant expression of ER-α (9/1 ratio of ER-α/ER-β expression), hence a well-accepted model for HDBC [29,30]. Therefore, T47D cell lines were utilised in the initial screening of the synthesised molecules for targeting BC. All the twenty one synthesised *N*-benzylated indole-benzimidazole derivatives (**5**) and N-H indole-benzimidazole derivatives (**8**) were evaluated for the antiproliferative activity using MTT assay at 1, 5, 25 μM concentration and bazedoxifene is taken as standard drug.

The anti-proliferative activity of most of the compounds was comparable to bazedoxifene (16.43 ± 0.94 μM). **5f, 5g, 8a, 8c** and **8f** showed marked anti-proliferative activity as compared to bazedoxifene. While other derivatives **5b, 5c, 5h, 8b, 8e, 8g** and **8h** have shown moderate antiproliferative activity (Table 1, Fig. 2). Compounds have shown dose dependent increase in anti-proliferative activity (Fig. 2). Upon analysing the structural features, it is evident that bromo substituted carbocylic D-ring (**5f,8f**) was found to be more active as compared to the bromo substituted heterocyclic D-ring (**5e, 5i, 8e, 8j**). For evaluating the cytotoxicity of the compound on the normal cell lines, all the compounds were screened on human PBMCs (Peripheral Blood Mononuclear Cells) using MTT assay, the results indicated that all the compounds were showing non-significant cytotoxicity even at higher concentration of 100 μM. The prerequisite requirement of SERM compound is to have ER-α binding affinity, therefore all the synthesised compounds were screened for determining their binding affinity towards ER-α. ER-α competitor assay kit (Polar Screen ER-α Competitor Assay Kit, Green, Life Technology) was used to determine the binding affinity.

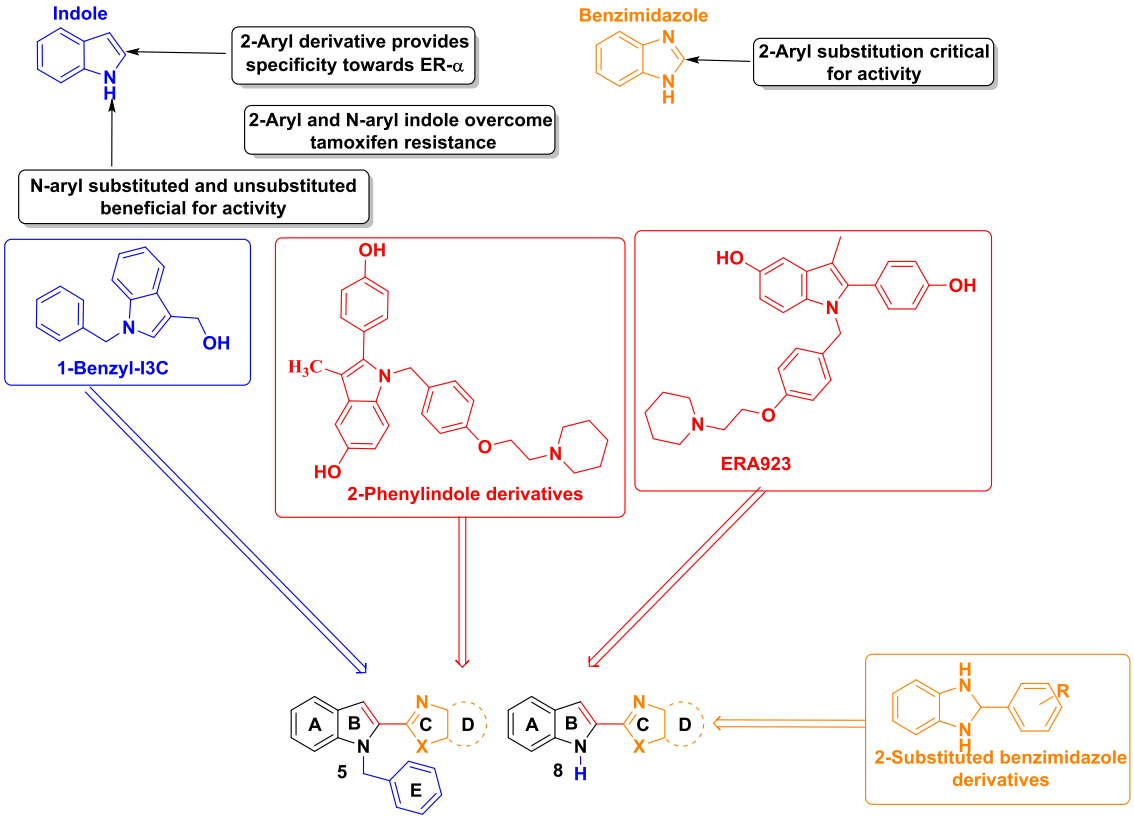

Fig. 1. Designing strategy of *N*-benzylated indole-benzimidazole hybrids (**5**) and N-H indole-benzimidazole hybrids (**8**).

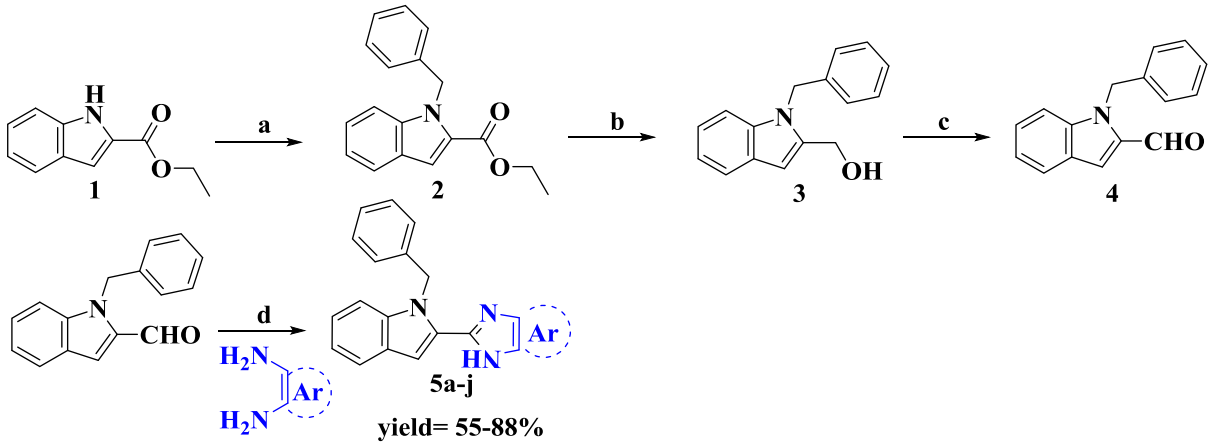

Scheme 1. Reagent and conditions (a) Benzyl bromide, KOH, DMSO, 1.5 h (b) $LiAlH_4$, dry THF, 0 °C, 30 min (c) activated MnO_2, dry CH_2Cl_2, r.t., 5 h (d) corresponding diamine, absolute ethanol, reflux 12 h.

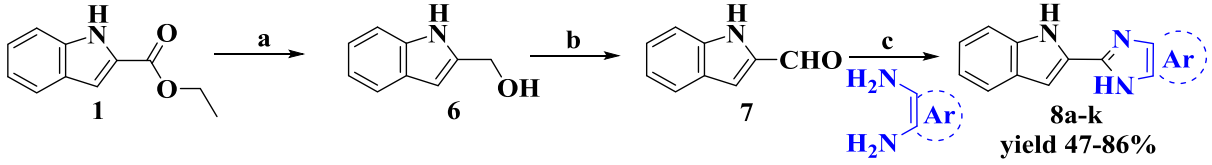

Scheme 2. Reagent and conditions (a) $LiAlH_4$, dry THF, 0 °C, 30 min (b), activated MnO_2, dry CH_2Cl_2, r.t., 5 h (c) corresponding diamine, absolute ethanol, reflux 12 h.

Table 1
Structure and biological evaluation of the synthesised indole-benzimidazole derivatives.

S.No	Code	Anti-proliferative activity using T47D cell line, $IC_{50} = \mu M$	Binding affinity with ER-α, $IC_{50} = nM$	Structure
1	5a	ND	387.37 ± 13.12	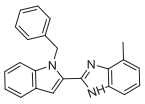
2	5b	21.8 ± 1.86	33.13 ± 5.37	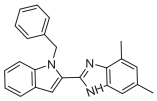
3	5c	21.45 ± 0.60	259.16 ± 26.42	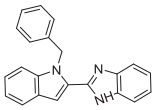
4	5d	ND	ND	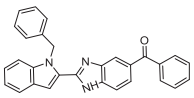
5	5e	ND	300.43 ± 10.40	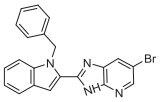
6	**5f**	**15.48** ± 0.10	**73.61** ± 3.25	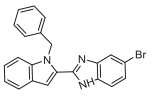
7	5g	13.44 ± 0.04	ND	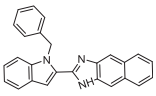
8	5h	22.5 ± 2.12	76.73 ± 6.35	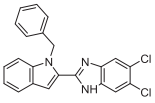
9	5i	ND	539.18 ± 34.79	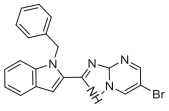
10	5j	ND	ND	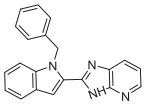
11	8a	8.9 ± 0.57	191.69 ± 14.99	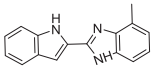
12	8b	24.8 ± 0.66	ND	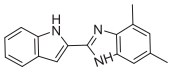
13	8c	6.2 ± 0.88	ND	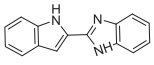
14	8d	ND	46.88 ± 0.95	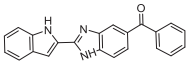
15	8e	21.03 ± 0.03	ND	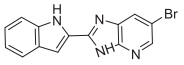
16	**8f**	**4.99** ± 0.60	**80.36** ± 7.02	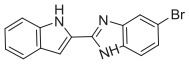

(*continued on next page*)

Table 1 (*continued*)

S.No	Code	Anti-proliferative activity using T47D cell line, IC_{50} = μM	Binding affinity with ER-α, IC_{50} = nM	Structure
17	8g	23.42 ± 0.07	ND	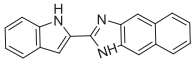
18	8h	20.47 ± 1.32	201.81 ± 5.19	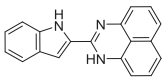
19	8i	21.16 ± 1.59	ND	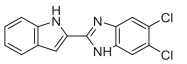
20	8j	24.4 ± 0.84	ND	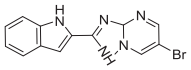
21	8k	ND	ND	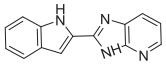

ND: Not determined as IC_{50} > 25 μM on T47D cell line and binding affinity IC_{50} > 1000 nM.

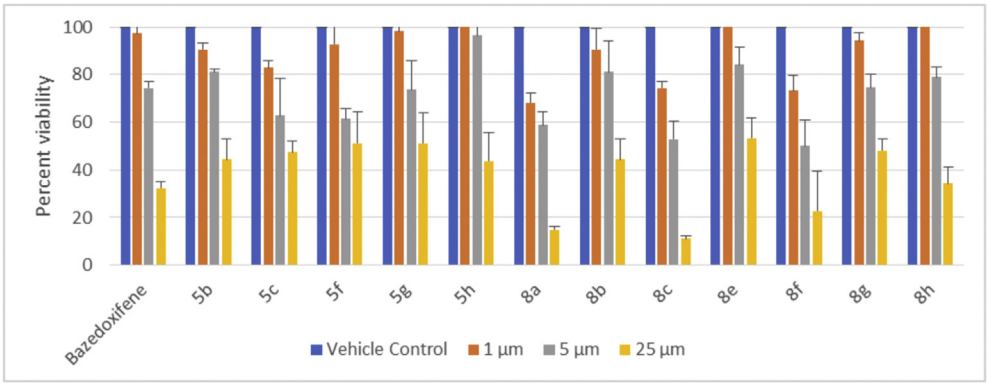

Fig. 2. MTT assay results showing potent and dose dependent anti-proliferative activity of synthesised compounds in comparison to bazedoxifene (positive control) on T47D cell line for 48 h.

The assay is based on the phenomenon that if the compound under investigation does not have affinity for the ER-α, then it will not be able to displace the Fluormone™ ES2 (fluorochrome tagged oestradiol) from the ER-α-Fluormone™ ES2 complex, thereby resulting in a high fluorescence. On the contrary, if the compound has a strong binding affinity for ER-α, then it will displace the Fluormone™ ES2 ligand from ER- α and resulting in a low fluorescence. This change in the fluorescence provides the relative affinity for ER-α. Bazedoxifene (31.71 ± 1.41 nM) was also included as standard in the study.

From the competitive binding assay, compounds **5f, 5h** and **8f** were found to be most potent binding affinity with IC_{50} value 73.61 ± 3.25, 76.73 ± 6.35 and 80.36 ± 7.02 nM respectively. Compounds **8a, 8h, 5c, 5e, 5a** and **5i** were having a moderate binding affinity with having IC_{50} 191.69 ± 14.99, 201.81 ± 5.19, 259.16 ± 26.42, 300.43 ± 10.40, 387.37 ± 13.12 and 539.18 ± 34.79 nM respectively (Table 1). Remaining nine compounds were having IC_{50} greater than 1000 nM. Upon comparative analysis of the anti-proliferative activity and ER-α binding affinity, it was found that, *N*-benzylation overall improves the activity and is important for ER-α binding. Upon comparing **5e** and **5f**, it was evident that if D-ring is heterocyclic in nature, then there will be reduction in the activity. Additionally, bromo substituted compounds (**5f, 8f**) are more active as compared to unsubstituted derivatives (**5c, 8c**).

Upon comparing the results from anti-proliferative assay and ER-α binding assay, some compounds (**5g, 8a, 8c**) were showing impressive anti-proliferative activity but a weak ER-α binding affinity. These compounds may be acting via alternate mechanism but not by targeting ER-α. Similarly, compound **5b, 5h** and **8d** were having a stronger binding affinity but were having weak anti-proliferative activity. Compounds **5f** and **8f** were selected for further studies as these compounds were showing both impressive antiproliferative activity as well as binding affinity towards the ER-α. Compounds **5f** and **8f** were escalated for confocal laser scanning microscopy (CLSM), quantitative RT-PCR and Western blotting for gene expression studies, from the group of *N*-benzylated indole-benzimidazole derivatives and N-H indole-benzimidazole derivatives.

It has been known that, ER-α is distributed in cytoplasm as well as nucleus [31]. In order to identify the distribution of the compounds **5f** and **8f** in T47D cell lines CLSM was performed. The compounds **5f** and **8f** have blue emission, so it was possible to detect the compound in T47D cells without tagging with an additional fluorochrome. The DAPI excitation-emission channel was used for evaluating its tendency to accumulate in T47D cell. The confocal images indicated selective targeting of cytosol and plasma membrane by the compounds **5f** and **8f** after 24 h incubation at 15 and 5 μM respectively. Both the compounds were able to cross the cellular bio-membrane, but not able to enter the nucleus region of

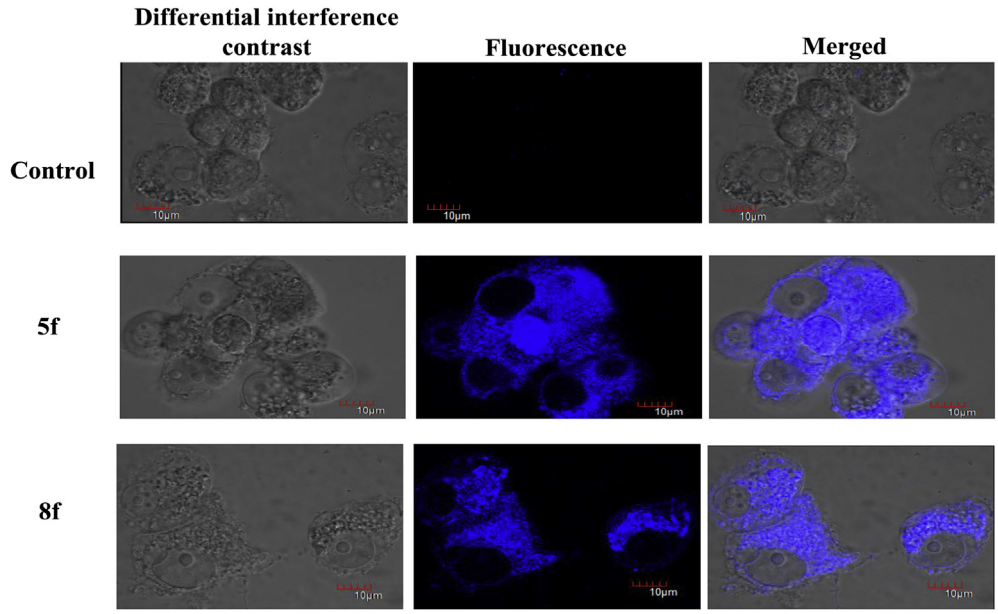

Fig. 3. CLSM analysis of T47D cells after treating the cells with compound **5f** and **8f** for 24 h and untreated cells as a control (Scale bar, 10 μM).

cancer cell thereby preventing any possible interaction at transcription level (Fig. 3). Thus, the confocal images undoubtedly confirm that the compounds are able to interact with the proteins present in the cytosol and plasma membrane. Thereby, obtained results of cell imaging, support our concept of anti-cancer activity by targeting cytoplasmic and membrane bound ER-α by the synthesized compounds.

There is elevated levels of mRNA for ER-α in BC progression [32]. If the drug molecules is active and have affinity for ER-α which will corresponds to decreased expression in mRNA levels of ER-α. Since, the compounds **5f** and **8f** have shown anti-proliferative activity and effective binding energy and were effectively able to target the cytoplasmic and membrane proteins of the T47D cell line. We examined the effect of **5f** and **8f** on the abundance of mRNA of ER-α in human T47D cell lines. The mRNA level of ER-α was determined by semi-quantitative RT-PCR using specific primers chosen from human DNA sequences and amplified in simpliAmp thermal cycler (Applied biosystem). The agarose gel image and the densitometric analysis (Fig. 4) imply that the expression of the mRNA of ER-α was completely inhibited in the cells treated with bazedoxifene, **5f** and **8f** T47D cell lines as compared to the control (untreated) cells. Thus, it can be concluded that compounds **5f** and **8f** decreases the expression of ER-α at the transcription level effectively similar to the standard bazedoxifene, thereby downregulating the signalling and transactivation pathways.

ER-α mediated metastasis has been associated with chemokine signalling, SRC3/AIB1, and mTOR pathway in non-genomic pathways, thereby inhibition of the ER-α protein can lead to enhanced management of BC [7]. Therefore, the semi-quantitative RT-PCR results were confirmed for evaluating the effect of compounds **5f** and **8f** on ER-α protein using Western blot analysis. The results obtained in Western blot can be correlated with the mRNA expression results obtained after semi-quantitative RT-PCR. The Western blot image and the densitometry analysis (Fig. 5) shows that high levels of ER-α protein was present in the untreated cells line. In contrast, expression of ER-α protein was reduced by 57.42% and 27.5% in the T47D cells treated with compound **5f** and **8f** respectively (Fig. 5). This signifies that, compound **5f** and **8f** not

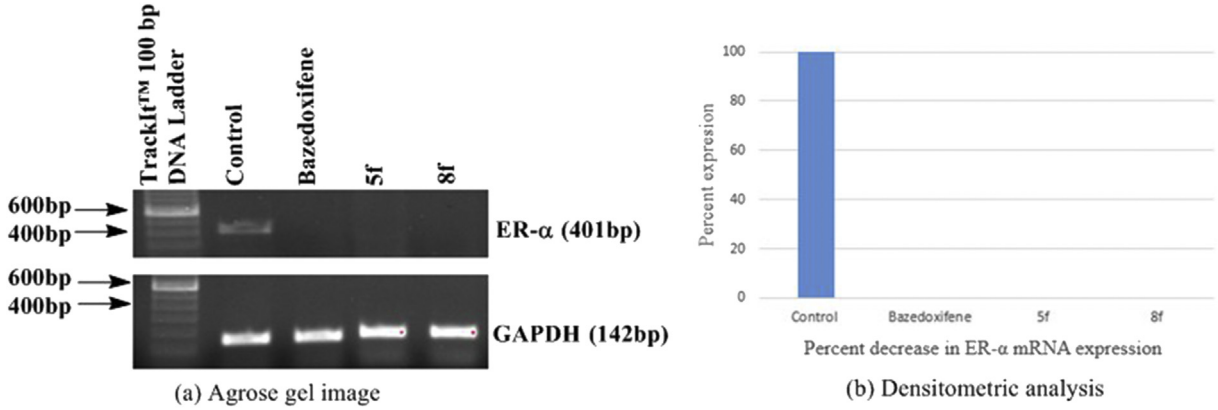

Fig. 4. mRNA expression profile of endogenous ER-α in the T47D cells line after treatment with bazedoxifene and synthesized compounds **5f** and **8f**. The cells were incubated with 15, 15 and 5 μM of bazedoxifene, **5f** and **8f** respectively for 48h. Data was normalised with GAPDH as an internal control, the results shown here are the representatives of three different experiments.

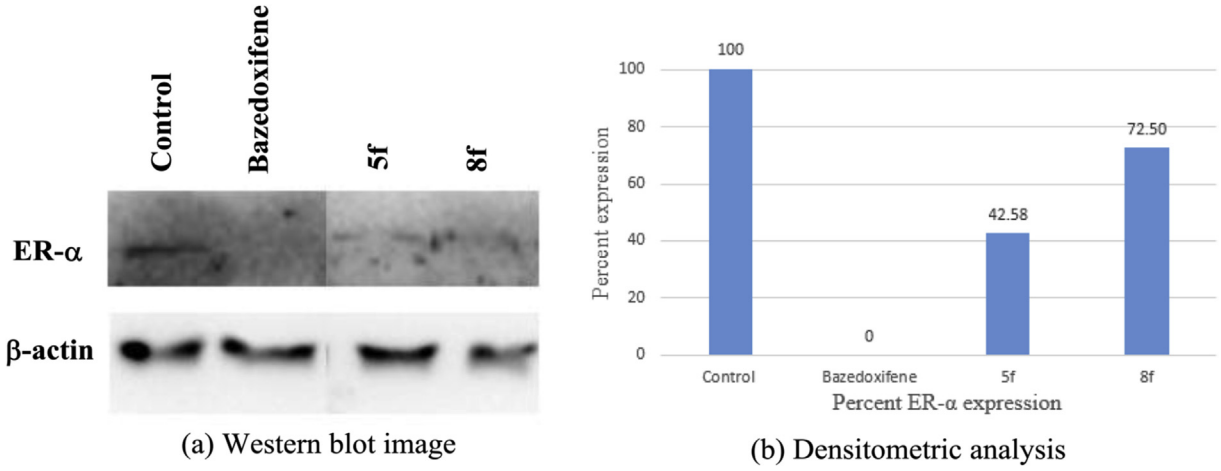

Fig. 5. Western blot analysis of endogenous ER-α protein in the T47D cells after treatment with bazedoxifene, **5f** and **8f**. The cells line was incubated with 15, 15 and 5 μM of bazedoxifene, **5f** and **8f** respectively for 48h. Data was normalised with β-actin as internal control, the results shown here are the representatives of three different experiments.

only downregulate the mRNA, but also reduces the protein levels of ER-α. Thus, synthesised compounds **5f** and **8f** exerts its anticancer activity in T47D cells ER-α and downregulating the expression of mRNA and protein of ER-α.

2.3. Structural investigation

The architecture of ER-α includes N-terminal hormone-independent transactivation domain, AF-1 (1–184), a highly conserved DNA-binding, ERE (185–250), a hinge region (251–310) which separates the DNA-binding domain from the ligand-binding domain (LBD), a LBD that contains the hormone binding pocket (311–551), and a second transactivation domain AF2 (311–595) in the C-terminus that is activated in response to ligand binding (Fig. 6a).

Molecular modelling study were carried out in an attempt to understand the molecular basis of interaction of compounds **5f** and **8f** with ER-α. As the rigid docking protocol possesses some pros and cons as it does not take account of the protein flexibility which has a significant impact on the binding modes and the docking protocol. Induced fit docking protocol is a ground-breaking protocol which includes protein flexibility and at the same time reducing the computational time without compromising with the accuracy in the prediction of favourable binding mode and conformation of ligand at the receptor site [33].

Using the available X-ray crystallographic structure 4XI3, for validation reasons co-crystalized bazedoxifene was also redocked in their native protein structure (Fig. 6b). The superimposition of the docked conformation and experimental structure of bazedoxifene shows that the docking model recapitulates the orientation of the native ligand in the active site, and the consistent interactions with the key amino acids of the binding cavity are formed with a

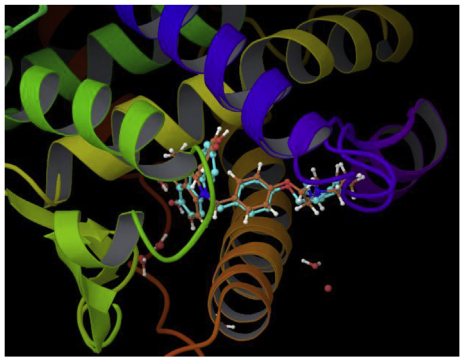

Fig. 7. Superposition of the docked structure of bazedoxifene (blue) with recrystallised experimental pose of bazedoxifene (orange) in 4XI3 with 0.02 Å rmsd. (For interpretation of the references to color in this figure legend, the reader is referred to the Web version of this article.)

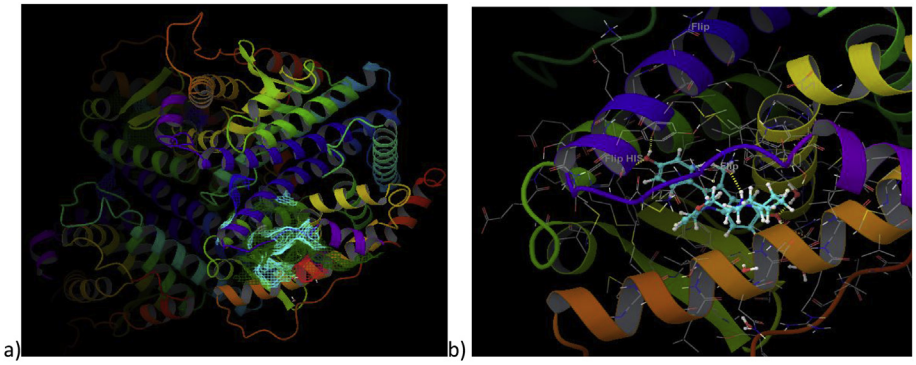

Fig. 6. (a) Crystal structure of ER-α with mesh representing the ligand binding domain, blue mesh represents hydrophilic region, green represent hydrophobic region, red positively charged region, dark blue represents negatively charged region, (b) bazedoxifene docked at the receptor site. (For interpretation of the references to color in this figure legend, the reader is referred to the Web version of this article.)

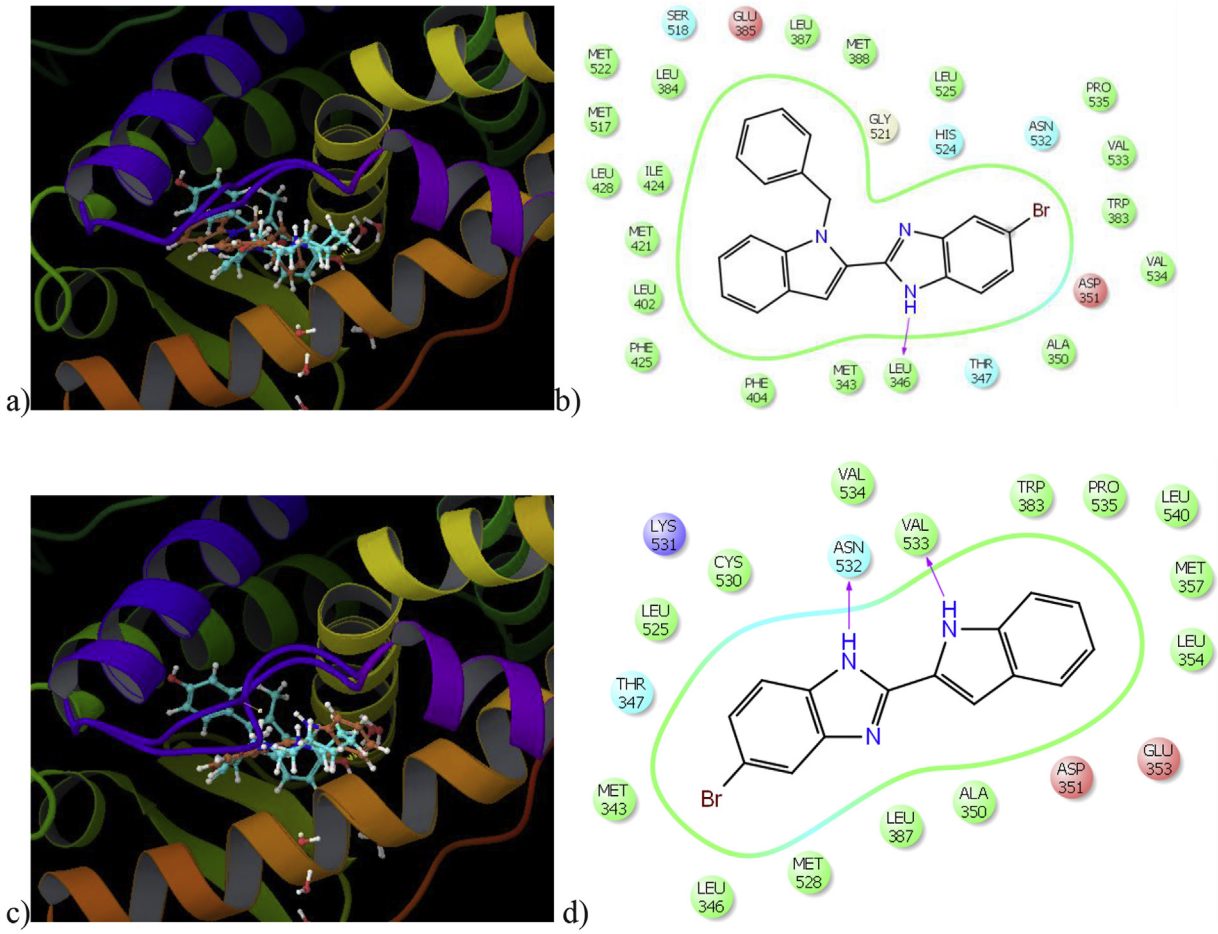

Fig. 8. (a) Superposition of bazedoxifene (blue) with compound **5f** (orange) at receptor site (b) ligand interaction diagram of compound **5f** (c) Superposition of bazedoxifene (blue) with compound **8f** (orange) at receptor site (d) ligand interaction diagram of compound **8f**. (For interpretation of the references to color in this figure legend, the reader is referred to the Web version of this article.)

ligand root mean square deviation of 0.02 Å compared with the crystal structure (Fig. 7).

Upon analysing the induced fit simulation, compound **5f** (Fig. 8a and b) and **8f** (Fig. 8c,d) have Van der Waals interaction with Met 343, Thr 347, Leu 349, Ala 350, Glu 353, Leu 354, Met 357 Trp 383, Leu 384, Glu 385, Leu 387, Met 388, Leu 391, Arg 394, Leu 402, Phe 404, Met 421, Ile 424, Phe 425, Leu 428, Met 517, Ser 518, Gly 521, Met 522, His 524, Leu 525, Met 528, Cys 530, Lys 531Val 534, Pro 535, Ser 536, Leu 539 Leu 540 and extensive H-bond integration with Asp 351, Leu 346, Asn 532, Val 533 present at the receptor site. Bazedoxifene, have also shown similar interaction with the amino acids at the receptor site (Fig. 6b). Thus, from the induced fit docking reveals that, compound **5f** and **8f** binds to ER-α in an antagonistic orientation similar to bazedoxifene and have tendency to form hydrophobic and hydrogen bond interaction lining the binding cavity (Fig. 8a and c). It can be concluded that both the compounds bind in antagonistic orientation similar with bazedoxifene. It has been observed that, during the induced fit docking, a number of residue adopt different conformations as compared to the experimental crystallographic structure of ER-α, code 4XI3. The ligand binding domain is composed of the helix 6–16 and coil 4–17 (311–551 aa) and most significant conformational change is found in coil 16 from helix 7,9 and 11. Further, in the recent reports the interaction with amino acid Leu 346 present in the helix 12 of the ER-α is found to be critical for the antagonistic activity [25], and compound **5f** is also exhibiting hydrogen bond interaction with Leu 346 by NH group (Fig. 8b). Hence, our rationally developed new indole-benzimidazole derivatives can serve as a contemporary potential lead in the developing SERMs.

It has been reported that the direct stimulation and cross talk of ER-α with other growth factors is an important mediator in BC proliferation. In our present investigation the rationally developed lead compounds **5f** and **8f**, exerts antiproliferation effect on T47D cells line by reducing the expression of ER-α at and mRNA level. This indicates that the functional integrity of the ER-α is disrupted by the treatment and it is a known fact that the ER-α is in a dynamic equilibrium in plasma membrane, cytoplasm and nucleoplasm, and therefore ER-α localised throughout these compartments is sought to be affected. This distortion of the active conformation of ER-α leads to restricted genomic as well as the non-genomic down signalling pathways involved in the BC progression. Moreover, by the initial SAR studies and docking analysis it can be inferenced that bulky side chain as in compounds **5d**, **5g** and **8g** leads to decreased in the activity which may be attributed due to stearic hindrance at the active site as indicated by the docking score (XP Lipophilic EvdW score in Supplementary Table 1). Presence of heterocyclic D-ring leads to the reduction in the activity (comparing **5e**, **5f**, **8e** and **8f**), which may be due to the decreased π-electron cloud due to presence of heteroatom in D-ring as compared to the benzene in D-ring. These reduced π-electron cloud leads to reduced hydrophobic interaction at the receptor site (XP Lipophilic EvdW score in Supplementary Table 1). The difference of the bromine atom in the

compound **5c**, **5f**, **8c**, **8f** serve as a basis for the differential antiproliferative and ER-α binding affinity. Herein, bromine serve as effective bioisostere for CF_3 [26]. Fluorine group present in fulvestrant occupies a "lipophilic hole" in the ER protein (XP Lipophilic EvdW score in Supplementary Table 1). The replaced fluorine group with the bromine, will not only tend to retain the metabolic stability but also improved the occupancy of lipophilic site present in the receptor.

3. Conclusion

In summary, we described the chemical synthesis and *in vitro* biological evaluation of novel indole-benzimidazole derivatives designed to inhibit ER-α and to act as SERMs. The *N*-benzylated indole-benzimidazole derivatives (**5**) and N-H indole-benzimidazole derivatives (**8**), were tested on estrogen-sensitive BC T47D cells and ER-α binding assay to screen the compounds bearing significant antiproliferative activity as well as high ER-α binding affinity. From the initial biological evaluation, it was evident that bromo substituted compounds (**5f**, **8f**) were most active compounds and thereby escalated for gene expression studies. Cell imaging results indicated that the cytotoxicity of compounds **5f** and **8f** was attributed by targeting cytoplasmic and membrane bound ER-α. From the semi-quantitative RT-PCR and Western blotting it was found that compounds **5f** and **8f** were able to decrease the mRNA and protein expression of the target ER-α, thereby decreasing the ER-α activity. Results from the molecular simulation that, compounds **5f** and **8f** form extensive hydrophobic and hydrogen bond interaction surrounding the binding cavity. Both the compounds interact with the similar amino acids neighboring the bazedoxifene hence, binds in the antagonistic confirmation similar to bazedoxifene. The result obtained in this study is promising considering that compound **5f** and **8f** represents the example of a indole-benzimidazole derivatives based inhibitor with core SERM activity. This suggests that these compounds could be used in future *in vivo* testing as a potent compound for the treatment of HDBC.

4. Experimental

4.1. Chemistry

4.1.1. General information

Starting materials and solvents were purchased from commercial suppliers and used without further purification. Reaction progress was monitored by TLC using silica gel 60 F254 (0.040e0.063 mm) with detection by UV. Silica gel 60–120 and 200–400 was used for column chromatography and flash chromatography respectively. ^{1}H NMR and ^{13}C NMR spectra were recorded on a Jeol 400 MHz and Bruker 400 MHz spectrometer using the residual signal of the deuterated solvent as internal standard. Splitting patterns are described as singlet (s), doublet (d), triplet (t) and broad (br); chemical shifts (d) are given in ppm. High-resolution mass spectra (HRMS) were recorded on an Q-ToF Micro Waters. Melting points were recorded on Stuart melting point apparatus (SMP-30) with open glass capillary tube and were uncorrected. IR spectra of compounds were recorded with KBr on a Bruker FT-IR spectrophotometer.

4.1.2. General procedure for the synthesis of intermediates *2*,*3* and *4*

Potassium hydroxide (4 mmol) was stirred in dried dimethyl sulfoxide (25 mL) for 10 min in a round-bottom flask. Ethyl 1*H*-indole-2-carboxylate **1** (1 mmol) was added to the solution and the mixture was stirred for 0.5 h. Benzyl bromide (1.3 mmol) was added to the stirring mixture. After the completion of the reaction (1.5 h) as monitored by TLC the reaction mixture was cooled to 0 °C. Product was extracted with ethyl acetate, the organic layer was washed using brine solution (40 mL). The combined organic layer was dried over anhydrous sodium sulfate, filtered, concentrated and was purified by isocratic flash column chromatography (petroleum ether: ethyl acetate = 9: 1, v/v) on silica gel (200–400) to get pure compound **2** with 95% yield.

For the synthesis of **3**, lithium aluminium hydride (2 mmol) was stirred in dry THF at 0 °C. Then **2** (1 mmol) was dissolved in THF and added drop wise to the solution of lithium aluminium hydride at 0 °C. Then, the mixture was slowly warmed to room temperature till the completion (0.5 h) of reaction as monitored by TLC. It was then cooled to 0 °C, 10% aqueous sodium hydroxide (20 mL) and 40 mL of water was added successively. Then reaction mixture was allowed to stir for 0.5 h, filtered through celite and washed with dry ethyl acetate, dried over anhydrous sodium sulfate, concentrated and purified by isocratic flash column chromatography (petroleum ether: ethyl acetate = 8: 2, v/v) on silica gel (200–400) to get pure compound **3** with 98% yield.

For the synthesis of **4**, compound **3** (1 mmol) was dissolved in dry CH_2Cl_2 (25 mL) was stirred briefly. Activated manganese dioxide (7.3 mmol) was added, stirred at room temperature for 4 h. Another portion of activated manganese dioxide (5.9 mmol) was added and stirred at room temperature for 0.5 h. After completion of the reaction, as monitored by TLC, the reaction mixture was filtered through Celite and washed with ethyl acetate, concentrated and purified by isocratic flash chromatography (petroleum ether: ethyl acetate 9.5: 0.5, v/v) on silica gel (200–400) to afford pure compound **4** with 70% yield.

4.1.3. General procedure for the synthesis of compounds ***5a-i***

Compound **4** (1 mmol) was taken in dissolved in ethanol in the presence of triethylamine, and appropriate diamine (1 mmol). The mixture was refluxed with stirring for 12 h and was monitored for completion using TLC. The reaction was generally completed in 12–15 h. After the completion of the reaction, excess of ethanol was removed under reduced pressure. The product was extracted using ethyl acetate and organic layer was washed with distilled water. The combined organic layer was dried over anhydrous sodium sulfate, filtered, concentrated and purified by isocratic flash column chromatography (petroleum ether: ethyl acetate = 9.5: 0.5, v/v) on silica gel (200–400) to afford pure *N*-benzylated indole-benzimidazole derivatives (**5a-i**) in 55–88% yields. The structures were confirmed by IR, NMR and HRMS.

*4.1.3.1. 2-(1-Benzyl-1H-indol-2-yl)-4-methyl-1H-benzo[d]imidazole (**5a**).* Dark brown solid; yield 76%; mp 107–108 °C; IR (KBr): 3244, 3056 (N-H stretch), 2919 (=C-H stretch), 2850, 1670 (C=N), 1614 (C=C), 1495 (N-H bending), 1295 (C-N stretch), 732 (N-H out of plane) cm^{-1}; ^{1}H NMR (400 MHz, DMSO) δ 9.91 (1H, s), 7.68–7.62 (1H, m), 7.51–7.45 (1H, m), 7.41–7.33 (1H, m), 7.26–7.15 (4H, m), 7.12–7.03 (4H, m), 6.97–6.91 (1H, m), 5.82 (1H, s), 5.60 (2H, s), 1.24 (3H, s). ^{13}C NMR (100 MHz, DMSO) δ 148.68, 139.50, 138.59, 137.89 (2C), 128.40, 128.28 (2C), 128.06, 127.08, 126.98, 126.77, 126.31 (2C), 126.09, 125.81, 124.35, 123.18, 122.12, 111.10, 110.22, 54.35, 17.34. HRMS(ESI):*m/z* calcd for $C_{23}H_{20}N_3^+$ $[M+H]^+$ 338.1657; found: 338.1657.

*4.1.3.2. 2-(1-Benzyl-1H-indol-2-yl)-4,6-dimethyl-1H-benzo[d]imidazole (**5b**).* Pale white solid; yield 68%; mp 155–156 °C; IR (KBr): 3394, 3059, 2920, 2857, 1623, 1582, 1495, 1332, 732 cm^{-1}; 1H NMR (400 MHz, DMSO) δ 9.88 (1H, br), 7.62–7.60 (1H, d, $J = 8$ Hz), 7.35–7.32 (1H, m), 7.24–7.20 (1H, m), 7.15–7.11 (5H, m), 7.07–7.05 (2H, m), 6.95 (1H, s), 6.88 (1H, s), 6.09 (2H, s), 2.53 (3H, s), 2.39 (3H,

s); ^{13}C NMR (100 MHz, CDCl3) δ 144.54, 138.87, 138.49, 133.02, 129.47, 128.64 (2C), 127.53, 127.10, 126.59 (2C), 125.02, 124.94, 123.47, 122.56, 121.21 (2C), 120.58, 110.78, 103.82, 99.99, 48.08, 21.65, 16.78. HRMS(ESI):*m/z* calcd for $C_{24}H_{22}N_3^+$ $[M+H]^+$ 352.1814; found: 352.1817.

*4.1.3.3. 2-(1-Benzyl-1H-indol-2-yl)-1H-benzo[d]imidazole (**5c**).* Yellow solid; yield 55%; mp 117–118 °C; IR (KBr):3474, 3374, 3028, 2925, 2867, 1620, 1599, 1492, 1351, 749 cm^{-1}; 1H NMR (400 MHz, CDCl3) δ 8.58 (1H, s), 7.72–7.70 (1H, d, *J* = 8 Hz), 7.32–7.29 (2H, m), 7.26–7.24 (2H, m), 7.22–7.20 (1H, m), 7.17–7.14 (1H, m) 7.07–7.05 (3H, m), 7.01–6.97 (2H, m), 6.72–6.69 (1H, m), 6.63–6.61 (1H, m), 6.01 (2H, s). ^{13}C NMR (100 MHz, CDCl3) δ 149.22, 142.18, 140.23, 138.85, 137.34, 135.73, 128.77 (2C), 127.58, 127.29, 127.02, 124.97 (2C), 122.02, 120.66, 118.32, 116.64, 115.27, 112.45, 110.19, 99.99, 48.37. HRMS(ESI):*m/z* calcd for $C_{22}H_{18}N_3^+$ $[M+H]^+$ 324.1501; found: 324.1501.

*4.1.3.4. (2-(1-benzyl-1H-indol-2-yl)-1H-benzo[d]imidazole-5-yl)(phenyl)methanone (**5d**).* Yellow solid; yield 84%; mp 157–158 °C; IR (KBr):3472, 3373, 3058, 2925, 1638, 1596, 1568, 1497, 1316, 719 cm^{-1}; ^{1}H NMR (400 MHz, $CDCl_3$) δ 8.77 (1H, s), 7.89–7.87 (3H, d, *J* = 8 Hz), 7.79–7.78 (1H, d, *J* = 4 Hz), 7.70–7.58 (4H, m), 7.46–7.39 (4H, m), 7.36–7.30 (2H, m), 7.26 (1H, s), 7.21–7.19 (2H, d, *J* = 8 Hz), 6.72–6.70 (1H, d, *J* = 8 Hz), 6.14 (2H, s).^{13}C NMR (100 MHz, CDCl3) δ 195.36, 150.35, 146.83, 140.33, 138.88, 138.82, 136.49, 135.24, 131.42, 131.37, 129.50 (2C), 128.79 (2C), 128.11 (2C), 127.16, 127.01, 126.92, 125.64 (2C), 125.28, 122.18, 120.74, 118.80, 113.40, 113.09, 110.06, 48.33. HRMS(ESI):*m/z* calcd for $C_{29}H_{22}N_3O^+$ $[M+H]^+$ 428.1763; found: 428.1769.

4.1.3.5. 2-(1-benzyl-1H-indol-2yl)-6-bromo-3H-imidazo[4,5,-b]pyridine (5e). Yellow solid; yield 80%; mp 127–128 °C; IR (KBr):3450, 3286, 2924, 2854, 1601, 1461, 1352, 1023, 750 cm^{-1}; ^{1}H NMR (400 MHz, $CDCl_3$) δ 8.52–8.50 (1H, d, *J* = 8 Hz), 7.73–7.71 (1H, m), 7.30–7.28 (2H, m), 7.26 (1H, s), 7.25–7.24 (1H, d, *J* = 4 Hz), 7.22–7.16 (2H, m), 7.08–7.07 (1H, m), 7.04–7.03 (2H, m), 6.73 (1H, s), 5.98 (2H, s), 3.57 (1H, br). ^{13}C NMR (100 MHz, $CDCl_3$) δ 149.94, 149.29, 143.38, 138.69, 136.16, 135.38, 129.76, 128.74 (2C), 127.16, 127.01, 125.67 (2C), 125.15, 120.84, 120.70, 120.57, 119.51, 112.89, 110.12, 48.29. HRMS(ESI):*m/z* calcd for $C_{21}H_{16}BrN_4^+$ $[M+H]^+$ 402.0480; found: 402.0480.

*4.1.3.6. 2-(1-Benzyl-1H-indol-2-yl)-5-bromo-1H-benzo[d]imidazole (**5f**).* Bright yellow solid; yield 67%; mp 121–122 °C; IR (KBr):3478, 3376, 3059, 2924, 1620, 1596, 1414, 1352, 1130, 750 cm^{-1}; ^{1}H NMR (400 MHz, $CDCl_3$) δ 8.52–8.50 (1H, d, *J* = 8 Hz), 7.73–7.71 (1H, m), 7.32–7.29 (1H, m), 7.26 (1H, s), 7.25–7.24 (1H, m), 7.22–7.20 (1H, m), 7.19–7.14 (2H, m), 7.11–7.07 (2H, m), 7.06–7.03 (2H, m), 6.84–6.80 (1H, m), 5.98 (2H, s), 3.58 (1H, br). ^{13}C NMR (100 MHz, $CDCl_3$) δ 150.01, 149.36, 136.23, 135.45, 135.25, 129.83, 128.80 (2C), 127.08, 125.74 (2C), 125.22, 122.12, 120.90, 120.77, 119.57, 117.79, 117.55, 116.33, 110.17, 104.40, 48.36. HRMS(ESI):*m/z* calcd for $C_{22}H_{17}BrN_3^+$ $[M+H]^+$ 402.0606; found: 402.0606.

*4.1.3.7. 2-(1-Benzyl-1H-indol-2-yl)-1H-naphtho[2,3-d]imidazole (**5g**).* Pale yellow solid; yield 76%; mp 169–170 °C; IR (KBr): 3477, 3376, 3051, 2925, 1630, 1598, 1464, 1351, 748 cm^{-1}; ^{1}H NMR (400 MHz, DMSO) δ 8.79 (1H, s), 7.72–7.70 (1H, d, *J* = 8 Hz), 7.65–7.62 (1H, d, *J* = 8 Hz), 7.47–7.41 (2H, m) 7.37–7.34 (2H, m), 7.29–7.25 (2H, m), 7.13–7.06 (4H, m), 7.05–6.99 (2H, m), 6.90 (1H, s), 6.70 (1H, s), 6.10 (2H, s). ^{13}C NMR (100 MHz, DMSO) δ 151.02, 138.52, 138.16, 137.77, 134.95, 128.36 (2C), 128.13 (2C), 127.39, 126.85, 126.76 (2C), 126.16 (2C), 125.74, 121.62 (2C), 121.42, 120.33, 119.31, 113.40, 112.95, 109.90, 99.85, 46.97. HRMS(ESI):*m/z* calcd for $C_{26}H_{20}N_3^+$ $[M+H]^+$ 374.1657; found: 374.1657.

*4.1.3.8. 2-(1-Benzyl-1H-indol-2-yl)-5,6-dichloro-1H-benzo[d]imidazole (**5h**).* Bright yellow solid; yield 58%; mp 119–120 °C; IR (KBr):3480, 3378, 3060, 2924, 1620, 1597, 1462, 1351, 1126, 750 cm^{-1}; ^{1}H NMR (400 MHz, $CDCl_3$) ^{1}H NMR (400 MHz, $CDCl_3$) δ 8.48 (1H, s), 7.74–7.72 (1H, d, *J* = 8 Hz), 7.32–7.29 (2H, m), 7.27–7.25 (1H, d, *J* = 8 Hz), 7.24–7.21 (1H, m), 7.19–7.16 (1H, m), 7.11 (1H, s), 7.03–7.01 (3H, m), 6.65 (1H, s), 5.95 (2H, s), 3.56 (1H, br).^{13}C NMR (100 MHz, $CDCl_3$) δ 150.14, 140.49, 138.68, 136.66, 135.08, 130.23 (2C), 128.84 (2C), 127.18, 127.13, 125.68 (2C), 125.53, 122.27, 120.88, 117.94, 113.75 (2C), 110.19, 99.99, 48.37. HRMS(ESI):*m/z* calcd for $C_{22}H_{16}$ $Cl_2N_3^+$ $[M+H]^+$ 392.0721; found: 392.0721.

*4.1.3.9. 2-(1-Benzyl-1H-indol-2-yl)-6-bromo-1,3a-dihydro-[1,2,4]triazolo[1,5-a]pyrimidine (**5i**).* Yellow solid; yield 88%; mp 170–172 °C; IR (KBr): 3452, 3385, 3031, 2924, 1602, 1553, 1453, 1352, 1023, 750 cm^{-1}; ^{1}H NMR (400 MHz, $CDCl_3$) δ 8.49 (1H, s), 7.92–7.91 (1H, d, *J* = 4 Hz), 7.75–7.73 (1H, d, *J* = 8 Hz), 7.33–7.32, (1H, m), 7.30–7.23 (4H, m), 7.20–7.16 (1H, m) 7.13 (1H, s), 7.03–7.01 (2H, d, *J* = 8 Hz), 5.95 (2H, s), 4.33 (1H, s), 1.79 (1H, s). ^{13}C NMR (100 MHz, DMSO) δ 153.25, 151.60, 146.06, 138.62, 134.83, 128.95 (2C), 127.26, 127.16, 125.88, 125.66 (2C), 125.24 (2C), 122.43, 121.04, 114.39, 110.26, 107.54, 48.43. HRMS(ESI):*m/z* calcd for $C_{20}H_{17}BrN_5^+$ $[M+H]^+$ 406.0667; found: 406.0667.

*4.1.3.10. 2-(1-Benzyl-1H-indol-2-yl)-3H-imidazo[4,5-b]pyridine (**5j**).* Yellow solid; yield 67%; mp 118–119 °C; IR (KBr): 3447, 3385, 3149, 2924, 1600, 1519, 1453, 1312, 750 cm^{-1}; ^{1}H NMR (400 MHz, DMSO) δ 8.72 (1H, s), 7.82–7.81 (1H, d, *J* = 8 Hz), 7.70–7.68 (1H, d, *J* = 8 Hz), 7.44–7.42 (1H, d, *J* = 8 Hz), 7.31–7.20 (6H, m), 7.14–7.06 (3H, m), 6.58–6.55 (1H, m), 6.06 (2H, s). ^{13}C NMR (100 MHz, DMSO) δ 153.26, 149.24, 144.22, 138.18, 137.04, 133.47, 129.73 (2C), 126.88 (2C), 125.27, 125.24, 124.25 (2C), 123.22, 121.07, 120.24, 118.82, 111.16, 108.74, 46.03. HRMS(ESI):*m/z* calcd for $C_{21}H_{17}N_4^+$ $[M+H]^+$ 325.1423; found: 325.1423.

*4.1.4. General procedure for the synthesis of intermediates **6** and **7***

For the synthesis of **6**, lithium aluminium hydride (2 mmol) was stirred in dry THF at 0 °C. Then **1** (1 mmol) was dissolved in THF and added drop wise to the solution of lithium aluminium hydride at 0 °C. Then, the mixture was slowly warmed to room temperature till the completion (0.5 h) of reaction as monitored by TLC. It was then cooled to 0 °C, 10% aqueous sodium hydroxide (20 mL) and 40 mL of water was added successively. Then reaction mixture was allowed to stir for 0.5 h, filtered through celite and washed with dry ethyl acetate, dried over anhydrous sodium sulfate, concentrated and purified by isocratic flash column chromatography (petroleum ether: ethyl acetate = 8: 2, v/v) on silica gel (200–400) to get pure compound **6** with 98% yield.

For the synthesis of **7**, compound **6** (1 mmol) was dissolved in dry CH_2Cl_2 (25 mL) was stirred briefly. Activated manganese dioxide (7.3 mmol) was added, stirred at room temperature for 4 h. Another portion of activated manganese dioxide (5.9 mmol) was added and stirred at room temperature for 0.5 h. After completion of the reaction, as monitored by TLC, the reaction mixture was filtered through Celite and washed with ethyl acetate, concentrated and purified by isocratic flash chromatography (petroleum ether: ethyl acetate 9.5: 0.5, v/v) on silica gel (200–400) to afford pure compound **7** with 70% yield.

*4.1.5. General procedure for the synthesis of compounds **8a-k***

Compound **7** (1 mmol) was taken in dissolved in ethanol in the presence of triethylamine, and appropriate diamine (1 mmol). The mixture was refluxed with stirring for 12 h and was monitored for

completion using TLC. The reaction was generally completed in 12–15 h. After the completion of the reaction, excess of ethanol was removed under reduced pressure. The product was extracted using ethyl acetate and organic layer was washed with distilled water. The combined organic layer was dried over anhydrous sodium sulfate, filtered, concentrated and purified by isocratic flash column chromatography (petroleum ether: ethyl acetate = 9.5: 0.5, v/v) on silica gel (200–400) to afford pure *N*-benzylated indole-benzimidazole derivatives (**8a-k**) in 47–86% yields. The structures were confirmed by IR, NMR and HRMS.

*4.1.5.1. 2-(1H-indol-2-yl)-4-methyl-1H-benzo[d]imidazole (**8a**).* Light yellow solid; yield 58%; mp 167–168 °C; IR (KBr):3384, 3055, 2918, 2850, 1621, 1569, 1395, 1342, 738 cm^{-1}; ^1H NMR (400 MHz, DMSO) δ 12.63 (1H, br), 11.77 (1H, br), 7.61–7.59 (1H, d, $J = 8$ Hz), 7.48–7.46(1H, d, $J = 8$ Hz), 7.39 (1H, br), 7.25 (1H, br), 7.15–7.01 (3H, m), 6.99–6.97 (1H, d, $J = 8$ Hz), 2.62 (3H, s). ^{13}C NMR (100 MHz, DMSO) δ 145.52 (2C), 136.87, 134.25 128.68 (2C), 127.81 (2C), 122.45, 121.87, 120.46, 119.47, 111.79 (2C), 101.61, 16.98. HRMS(ESI):*m/z* calcd for $C_{16}H_{14}N_3^+$ $[M+H]^+$ 248.1188; found: 248.1188.

*4.1.5.2. 2-(1H-indol-2-yl)-4,6-dimethyl-1H-benzo[d]imidazole (**8b**).* Pale yellow solid; yield 69%; mp 134–135 °C; IR (KBr): 3385, 3056, 2919, 1596, 1572, 1435, 1395, 756 738 cm^{-1}; ^1H NMR (400 MHz, DMSO) δ 12.54 (1H, br), 11.73 (1H, br), 7.60–7.58 (1H, d, $J = 8$ Hz), 7.48–7.46 (1H, d, $J = 8$ Hz), 7.15–7.11 (3H, m), 7.04–7.00 (1H, m), 6.82 (1H, s), 2.57 (3H, s), 2.41 (3H, s). ^{13}C NMR (100 MHz, DMSO) δ 144.88, 137.04 (2C), 128.88 (2C), 127.83 (2C), 123.61, 122.32, 120.39, 119.42 (2C), 111.81 (2C), 101.27, 21.29, 16.93. HRMS(ESI):*m/z* calcd for $C_{17}H_{16}N_3^+$ $[M+H]^+$ 262.1344; found: 262.1344.

*4.1.5.3. 2-(1H-indol-2-yl)-1H-benzo[d]imidazole (**8c**).* Pale yellow solid; yield 65%; mp 250–252 °C; IR (KBr): 3589, 3435, 3055, 2922, 1601, 1572, 1401, 1329, 737 cm^{-1}; ^1H NMR (400 MHz, DMSO) δ 11.09 (1H, br), 10.67 (1H, br), 7.46–7.39 (1H, m), 7.31–7.26 (4H, m), 7.13–7.10 (3H, m), 5.87 (1H, s). ^{13}C NMR (100 MHz, DMSO) δ 146.63, 145.88, 142.21, 137.54, 128.11, 124.04, 123.38 (2C), 121.22, 120.69, 120.56, 112.09, 111.79, 111.21, 101.79. HRMS(ESI):*m/z* calcd for $C_{15}H_{12}N_3^+$ $[M+H]^+$ 234.1031; found: 234.1031.

*4.1.5.4. (2-(1H-indol-2-yl)-1H-benzo[d]imidazole-5-yl)(phenyl) methanone (**8d**).* Yellow solid; yield 85%; mp 199–200 °C; IR (KBr): 3433, 3328, 3053, 2922, 1591, 1553, 1503, 1421, 1318, 738 cm^{-1}; ^1H NMR (400 MHz, DMSO) δ 11.56 (1H, s), 8.66 (1H, s), 7.75–7.74(1H, d, $J = 4$ Hz), 7.70–7.68 (2H, d, $J = 8$ Hz), 7.61–7.59 (1H, d, $J = 8$ Hz),7.57–7.55 (1H, d, $J = 8$ Hz), 7.51–7.46 (2H, m), 7.44–7.42 (1H, d, $J = 8$ Hz) 7.24–7.20 (1H, t, $J = 8$ Hz), 7.06–7.02 (1H, t, $J = 8$ Hz), 6.95 (1H, s), 6.79–6.77 (1H, d, $J = 8$ Hz), 6.31 (1H, s). ^{13}C NMR (100 MHz, DMSO) δ 193.91, 149.37, 146.39, 146.34, 138.76, 137.62, 136.24, 133.09, 131.11, 130.91 (2C), 128.81, 127.83, 127.76, 124.29, 124.01, 121.34, 119.44, 117.65, 112.86, 111.43, 108.60. HRMS(ESI):*m/z* calcd for $C_{22}H_{16}N_3O^+$ $[M+H]^+$ 338.1293; found: 338.1293.

*4.1.5.5. 6-Bromo-2-(1H-indol-2-yl)-3H-imidazo[4,5-b]pyridine (**8e**).* Brown solid; yield 67%; mp 171–172 °C; IR (KBr): 3421, 3299, 2924, 2854, 1724, 1587, 1419, 1327, 1122, 750 cm^{-1}; ^1H NMR (400 MHz, DMSO) δ 11.66 (1H, s), 9.18 (1H, s), 7.64–7.62 (1H, d, $J = 8$ Hz), 7.60 (1H, s), 7.44–7.42 (1H, d, $J = 8$ Hz), 7.28–7.25 (1H, m), 7.11–7.10 (1H, d, $J = 4$ Hz), 7.08–7.04 (2H, m). ^{13}C NMR (100 MHz, DMSO) δ 152.41, 150.01, 139.70, 138.04, 135.89, 135.22, 129.60, 127.83, 124.98 (2C), 121.77, 119.74, 111.55, 110.72. HRMS(ESI):*m/z* calcd for $C_{14}H_9BrN_4Na^+$ $[M+Na]^+$ 334.9908; found: 334.9907.

*4.1.5.6. 5-Bromo-2-(1H-indol-2-yl)-1H-benzo[d]imidazole (**8f**).* Yellow solid; yield 47%; mp 187–188 °C; IR (KBr): 3385, 3060, 2956, 2624, 1614, 1572, 1392, 1322, 1148, 749 cm^{-1}; ^1H NMR (400 MHz, DMSO) δ 12.78 (1H, br), 11.72 (1H, s), 7.64–7.52 (2H, m), 7.47–7.39 (1H, m), 7.33–7.26 (1H, m), 7.22–7.20 (1H, m), 7.13–7.06 (1H, m), 7.01–6.86 (2H, m). ^{13}C NMR (100 MHz, DMSO) δ 147.34, 137.18 (2C), 136.84, 127.93, 127.70, 125.93,120.74, 120.58, 120.01, 119.65, 119.58, 119.08, 111.81, 102.11. HRMS(ESI):*m/z* calcd for $C_{15}H_{11}BrN_3^+$ $[M+H]^+$ 312.0136; found: 312.0131.

*4.1.5.7. 2-(1H-indol-2-yl)-1H-naphtho[2,3-d]imidazole (**8g**).* Yellow solid; yield 70%; mp 187–188 °C; IR (KBr):3422, 3050, 2922, 1628, 1588, 1416, 1276, 749 cm^{-1};^1H NMR (400 MHz, DMSO) δ 11.62 (1H, s), 8.68 (1H, s), 7.55 (1H, br), 7.47 (1H, s), 7.41–7.37 (2H, m), 7.28 (1H, br), 7.16–7.13 (1H, m), 6.98–6.88 (4H, m), 5.44 (1H, br). ^{13}C NMR (100 MHz, DMSO) δ 148.47, 138.37, 137.81, 129.90, 127.72, 127.49, 126.67, 125.17 (2C), 124.88, 124.58, 124.17 (2C), 121.43, 121.25, 111.70 (2C), 109.05, 99.30. HRMS(ESI):*m/z* calcd for $C_{19}H_{14}N_3^+$ $[M+H]^+$ 284.1188; found: 284.1188.

*4.1.5.8. 2-(1H-indol-2-yl)-1H-perimidine (**8h**).* Reddish brown solid; yield 71%; mp 162–163 °C; IR (KBr): 3384, 3047, 2924, 1600, 1562, 1481, 1289, 750 cm^{-1}; ^1H NMR (400 MHz, DMSO) δ 11.00 (1H, s), 9.75(1H, s), 7.41–7.39 (1H, d, $J = 8$ Hz), 7.32–7.30 (1H d, $J = 8$ Hz), 7.09–7.05 (2H, t, $J = 8$ Hz), 7.01–6.97 (1H, t, $J = 8$ Hz), 6.94–6.88 (2H, m), 6.48–6.47 (3H,m) 6.42 (s, 1H). ^{13}C NMR (100 MHz, DMSO) δ 142.21 (2C), 138.72, 136.13, 134.25, 127.06, 126.60 (2C), 121.16 (2C), 119.87, 118.80 (2C), 115.69, 112.74, 111.25, 104.68 (2C), 100.32. HRMS(ESI):*m/z* calcd for $C_{19}H_{14}N_3^+$ $[M+H]^+$ 284.1188; found: 284.1188.

*4.1.5.9. 5,6-Dichloro-2-(1H-indol-2-yl)-1H-benzo[d]imidazole (**8i**).* Dark green solid; yield 85%; mp; IR (KBr): 3421, 2955, 2917, 1593, 1556, 1417, 1297, 1122, 739 cm^{-1}; ^1H NMR (400 MHz, DMSO) δ 11.92 (1H, s), 11.61 (1H, s), 8.67 (2H, s), 7.62–7.60 (1H, d, $J = 8$ Hz), 7.44–7.42 (1H, d, $J = 8$ Hz), 7.24–7.22 (1H, m), 7.06–7.03 (1H, m), 6.88 (1H, s). ^{13}C NMR (100 MHz, DMSO) δ 148.46, 146.98, 144.63, 137.73, 137.34, 136.18, 133.49, 129.25, 127.75, 124.15, 119.51, 117.05, 114.74, 111.53, 108.98. HRMS(ESI):*m/z* calcd for $C_{15}H_{10}Cl_2N_3^+$$[M+H]^+$ 302.0252; found: 302.0252.

*4.1.5.10. 6-Bromo-2-(1H-indol-2-yl)-1,3a-dihydro-[1,2,4]triazolo[1,5-a]pyrimidine (**8j**).* Yellow solid; yield 86%; mp 162–163 °C; IR (KBr): 3480, 3300, 3058, 2921, 1602, 1553, 1448, 1330, 1123, 736 cm^{-1} 1H NMR (400 MHz, DMSO) δ 11.65 (1H, s), 8.74 (1H, s), 7.88 (1H, s), 7.67 (1H, s), 7.63–7.61 (1H, d, $J = 8$ Hz), 7.44–7.42 (1H, d, $J = 8$ Hz), 7.25–7.21 (1H, t, $J = 8$ Hz), 7.06–7.02 (1H, t, $J = 8$ Hz), 6.99 (1H, s), 6.41 (1H, s) ^{13}C NMR (100 MHz, DMSO) δ 155.05, 149.02, 145.80, 137.84, 136.04, 130.25, 127.73, 124.23, 121.55, 119.60, 111.60, 109.47, 105.39. HRMS(ESI):*m/z* calcd for $C_{13}H_{10}BrN_5^+$$[M]^+$ 315.0120; found: 315.0120.

*4.1.5.11. 2-(1H-indol-2-yl)-3H-imidazo[4,5-b]pyridine (**8k**).* Yellow solid; yield 49%; mp 168–169 °C; IR (KBr): 3392, 3056, 2955, 2924, 1601, 1526, 1426, 1325, 734 cm^{-1}; ^1H NMR (400 MHz, DMSO) δ 11.87 (1H, s), 10.87 (1H, s), 8.14–8.12 (1H, d, $J = 8$ Hz), 7.81–7.79 (1H, d, $J = 8$ Hz), 7.77–7.75 (1H, d, $J = 8$ Hz), 7.67–7.65 (1H, d, $J = 8$ Hz), 6.86–6.82 (1H, t, $J = 8$ Hz), 6.71–6.67 (2H, m), 5.54 (1H, s). ^{13}C NMR (100 MHz, DMSO) δ 154.05, 141.01, 137.79, 136.41, 135.75, 132.67, 129.85, 127.84, 123.37, 122.99, 121.99, 119.23, 117.13, 114.05. HRMS(ESI):*m/z* calcd for $C_{28}H_{20}N_8Na^+$ $[M+Na]^+$ 491.1709; found: 491.1709.

4.2. Biological assay methods

4.2.1. Culturing and maintaining of cancer cell line

Human BC cell line T47D were procured from National Centre for Cell Sciences (NCCS) Pune. T47D cells were grown in the Roswell Park Memorial Institute-1640 (RPMI-1640) medium supplemented with 10% heat inactivated (30 min at 56 °C) FBS (Fetal Bovine Serum), 1X penicillin and streptomycin in a tissue culture flask at 37 °C in a humidified atmosphere of 5% CO_2 incubator. At 70–80% confluence the cells were trypsinized using 1X trypsin-EDTA and sub-cultured in a new sterile tissue culture flask for further experiments.

4.2.2. Anti-proliferative activity

The anti-proliferative activity of the compounds was evaluated using the MTT assay. It is a colorimetric assay for assessing cell metabolic activity. Viable cells with active metabolism convert the MTT into a purple coloured formazan product with an absorbance maximum near 570 nm. When cells die, they lose the ability to convert MTT into formazan, thus color formation serves as a useful and convenient marker of only the viable cells. Human BC cell line T47D were seeded in 96 wells plate at cell density 1×10^4 per well and after 24 h, cells were treated with different concentration of synthesized compounds (1, 5, 25 μM) and incubated for 48 h in FBS-free media. MTT solution (final concentration of MTT was 0.5 mg/ml) was added followed by incubation for 4 h at 37 °C. After 4 h; the purple color farmazone crystals were solubilized using 100 μl of acidified DMSO with 0.6% acetic acid and absorbance was measured at both 570 nm and 620 nm. The absorbance reading is directly proportional to a number of living cells [34]. The cell viability of each group was calculated with their respective control.

4.2.3. Human peripheral blood mononuclear cells (PBMCs) culture and MTT assay

Majority of the chemotherapeutic agents available having a side effect of inducing apoptosis in the normal cell along with the cancer cells. Therefore, in order to analyze the side effect of the compounds on the normal cells at higher concentrations, human PBMC was cultured and MTT assay was performed. Fresh blood was drawn from healthy individual as per the protocol no. CUPB/cc/14/IEC/4483 approved by Institutional Ethics Committee of Central University of Punjab, Bathinda. The protocol used was standard operating procedure, provided by Institutional Ethics Committee of Central University of Punjab according to guidelines issued by Indian Council of Medical Research (ICMR), Govt. of India. PBMC were isolated from whole blood discarding the RBCs after treatment with RBC lysis buffer. The PBMCs were counted on the automated cell counter (Invitrogen). The cells were then suspended in RPMI-1640 media supplemented with 10% fetal bovine serum (FBS), 1 × antibiotic solution and incubated at 37 °C in a humidified atmosphere of 5% CO_2. Approximately 10^4 cells were seeded in each well of the 96 well plate. MTT assay was performed as described in section 4.2.2.

4.2.4. Estrogen receptor competitive binding assay

A stock solution of each compound was serially diluted using DMSO, and the 40 μL of each concentration was transferred to the assay plate (Grenier, 384-well high volume flat bottom) followed by adding 40 μL human recombinant ER-α/fluoromone TM complex solution. After mixing and allowing at least 2-h incubation at room temperature with light protection of the reagents. The fluorescence of each well was measured using the Synergy 2 multi-mode microplate reader (BioTek) with 535 nm excitation filters and 590 nm emission filters. Three controls were included in the assay: (1) assay maximum polarization control (40 μL of ER/fluoromone complex solution and 40 μL of ER green assay buffer with 4% DMSO, provides maximum polarization value for assay); (2) assay minimum polarization control (40 μL of ER/fluromone complex solution and 40 μL of oestradiol (20 mM), provides bottom baseline); (3) free fluoromone tracer control (40 μL Fluoromone tracer and 40 μL of ER green assay buffer with 4% DMSO, provides absolute minimum polarization value). The polarization values were normalized to percent inhibition using the following equation.

$$I\% = (A_0 - A)/(A_0 - A_{100}) \times 100$$

I% = the percent inhibition, A_0 = Absorbance at 0% inhibition, A_{100} = Absorbance at 100% inhibition, and A = observed Absorbance value.

The percent inhibition values are plotted against the concentration of test compounds and analysed by a non-linear regression curve fitting. The concentration of the test compounds needed to displace half of the bond ligand equals IC_{50} of the test compound.

4.2.5. Confocal microscopy

Cell imaging is an important technique for localisation of the compound inside the cell. As the ER is located on the plasma membrane, cytosol and nucleoplasm, live cell imaging enables to track the compound and site of action. Cells were seeded on sterile glass coverslip at 5×10^4 cells/ml in a 6 wells plate. After 24 h of seeding the cells were treated with 15 and 5 μM of **5f** and **8f** respectively for 48 h after that cells were washed with 1X PSB. After that cells were fixed with 2% formaldehyde solution for 10 min in dark, again cells were washed thrice with 1X PBST. Then cells were mounted on glass cover by using mounting media. Cells were visualized and image was captured under an Olympus FV1200 Laser Scanning Microscopes fluorescence confocal microscope, the captured image was analyzed with Olympus Fluoview software of Olympus version 4.2a.

4.2.6. Preparation of total cell lysates

To determine target specificity of the compounds, there is a need to determine the expression of target proteins. Cell lysates were prepared from both treated and untreated cells of T47D Briefly, cells were first rinsed twice gently with ice-cold 1X PBS, then 300–500 μL of modified RIPA buffer [50 mM TrisHCl (pH 7.4), 150 mM NaCl, 1 mM EDTA, 1% NP-40, and protease inhibitor cocktail (1 μL per 100 μL of lysis buffer)] was added per plate, kept on ice for 5 min, and cells were mechanically scraped using plastic cell scraper and cell suspension was transferred into pre-cooled 1.5 mL micro centrifuge tube [35]. Following centrifugation, the pellet was re-suspended in the cell lysis buffer with intermediate vortexing every 5min for 20 min at 4 °C. Then, the mixture was centrifuged at 12,000 g for 20 min at 4 °C. The supernatant was collected in pre-chilled sterile micro centrifuge tubes and stored at −20 °C for further experiments. The concentration of total protein in this supernatant was estimated by using standard Bradford method with BSA as standard [36].

4.2.7. Western blot analysis

50 μg of total protein sample were resolved on 10% denaturation SDS-PAGE and transferred to a nitrocellulose membrane. Membranes were blocked for 1 h with 5% nonfat dry milk (NFDM) in 1X PBST. All antibody dilutions were made in 2.5% NFDM-PBST. Membranes were incubated (4 °C overnight) with primary antibodies of rabbit α-ER- α (HC-20. Membranes were washed with PBST, incubated with horseradish peroxidase-conjugated secondary antibody (Invitrogen) for 1 h. The image was captured by using Bio-Rad ChemiDoc™ MP imaging system after applying enhanced chemiluminescence (Clarity™ Western ECL Substrate of Bio-Rad)

and densitometric analysis was done using Image Lab™ software of Bio-Rad version 5.2.

4.2.8. Total RNA isolation and cDNA synthesis

Total RNA was isolated from T47D cells from both treated and untreated cells by using TRIzol® (Invitrogen), and followed the manufacturer instructions and finally RNA pellet was resuspended in nuclease free water. Quality of isolated RNA was checked on NanoDrop 2000c (Thermo Scientific) followed by denaturing agarose gel. Traces of DNA contamination was removed by treating the total isolated RNA with DNA-free™ DNA Removal Kit (Invitrogen), and followed the manufacturer instructions. Again, the quality of DNA free RNA was checked, followed by synthesis of first strand of cDNA by using the SuperScript™ IV First-Strand Synthesis System (Invitrogen) as per the instructions by the manufacturer.

4.2.9. RT-PCR

cDNA was used as a template for the PCR reaction with gene-specific primer pairs of ER-α (5′ GTGCCTGGCTAGAGATCCTG 3′, 3′ GATGTGGGAGAGGATGAGGA 5′) along with a housekeeping gene (GAPDH) as a loading control. The PCR product was separated on 1.2% agarose gel containing ethidium bromide (EtBr) along with 100bp DNA ladder of Invitrogen (Tracklt™ 100 bp DNA ladder). The gel image was taken by using Bio-Rad Gel Doc™ XR system and densitometric analysis was done using Image Lab™ software of Bio-Rad version 5.2.

4.3. Induced fit docking

The 2D structure of ligands were constructed using the maestro 9.6 software and saved in sdf format (standard data format). The 2D structures were converted to the 3D structure using the Ligprep module of Maestro 9.6. This module adds hydrogens, eliminates any discrepancies between bond length and angle. The 3-dimensional and X-ray structure coordinates of ER-α was obtained from protein data bank with PDB id code 4XI3 (www.rcsb.org). Protein preparation wizard of maestro 9.6 was used for the protein preparation. Protein preparation begins with the application of Impact molecular mechanics program for correcting the bond orders, adding missing hydrogens and removing the crystallized waters that are not present in the active site.

A Truncated Newton Conjugate Gradient (TNCG) minimization was performed using the OPLS-2005 force field. IFD protocol utilizes a combination of Glide (grid-based ligand docking with energetics) rigid docking and prime (protein structure prediction). IFD consisted of three-step procedure for sampling side chain conformations and predicting ligand-residue orientations. In the first step, side chain conformation is generated, all previously mutated side chains were back mutated concurrently into a random rotamer state obtained from the rotamer libraries developed by Xiang and Honig. In the second step after the conformation generation, each side chain is minimized successively (<0.001 kcal mol rms gradient) while all other side chains are remaining fixed. Minimization of individual side chains was repeated sequentially for all back mutated residues until convergence was reached. In the third step, a TNCG minimization performed to resolve steric clashes. The target substrates obtained after the final step within a 40 kcal/mol window were redocked into the induced fit structures. GlideXP (Glide Extra precision) with vdW scaling 0.8 was employed for all docking. 20 poses were requested for the redocking and ranked based on the GlideXP score. Application of the IFD protocol produced an individual ensemble for ER-α complexes, which clustered for each compound under investigation. The cluster for the top scoring indole alkaloid was analysed.

Acknowledgement

Authors are grateful to Department of Science and Technology, New Delhi, India (SB/FT/CS-006/2012) for providing financial assistance during the course of the work. Ramit Singla acknowledge CSIR-India for the award of SRF [09/1051 (006)/2016-EMR-1]. Authors acknowledge Mr. Ashish Pandey of CIL in Central University of Punjab, for outstanding work on CLSM. Authors are also thankful to the Honourable Vice - Chancellor for providing the necessary facilities at Central University of Punjab, Bathinda, India.

Appendix A. Supplementary data

Supplementary data related to this article can be found at https://doi.org/10.1016/j.ejmech.2018.01.051.

References

[1] N.E.I. Guissi, H. Li, Y. Xu, F. Semcheddine, M. Chen, Z. Su, Q. Ping, Mitoxantrone- and folate-TPGS2k conjugate hybrid micellar aggregates to circumvent toxicity and enhance efficiency for breast cancer therapy, Mol. Pharm. 14 (2017) 1082–1094.
[2] C. Ouellet, R. Maltais, É. Ouellet, X. Barbeau, P. Lagüe, D. Poirier, Discovery of a sulfamate-based steroid sulfatase inhibitor with intrinsic selective estrogen receptor modulator properties, Eur. J. Med. Chem. 119 (2016) 169–182.
[3] T. Shoda, M. Kato, R. Harada, T. Fujisato, K. Okuhira, Y. Demizu, H. Inoue, M. Naito, M. Kurihara, Synthesis and evaluation of tamoxifen derivatives with a long alkyl side chain as selective estrogen receptor down-regulators, Bioorg. Med. Chem. 23 (2015) 3091–3096.
[4] J.S. Lewis-Wambi, H. Kim, R. Curpan, R. Grigg, M.A. Sarker, V.C. Jordan, The selective estrogen receptor modulator bazedoxifene inhibits hormone-independent breast cancer cell growth and down-regulates estrogen receptor α and cyclin D1, Mol. Pharmacol. 80 (2011) 610–620.
[5] M.J. Duffy, Estrogen receptors: role in breast cancer, Crit. Rev. Clin. Lab. Sci. 43 (2006) 325–347.
[6] A.W. Welsh, D.R. Lannin, G.S. Young, M.E. Sherman, J.D. Figueroa, N.L. Henry, L. Ryden, C. Kim, R.R. Love, R. Schiff, Cytoplasmic estrogen receptor in breast cancer, Clin. Canc. Res. 18 (2012) 118–126.
[7] C.K. Osborne, R. Schiff, Mechanisms of endocrine resistance in breast cancer, Annu. Rev. Med. 62 (2011) 233–247.
[8] J. Dandriyal, R. Singla, M. Kumar, V. Jaitak, Recent developments of C-4 substituted coumarin derivatives as anticancer agents, Eur. J. Med. Chem. 119 (2016) 141–168.
[9] S.J. Han, K. Begum, C.E. Foulds, R.A. Hamilton, S. Bailey, A. Malovannaya, D. Chan, J. Qin, B.W. O'Malley, The dual estrogen receptor α inhibitory effects of the tissue-selective estrogen complex for endometrial and breast safety, Mol. Pharmacol. 89 (2016) 14–26.
[10] F. Payton-Stewart, S.L. Tilghman, L.G. Williams, L.L. Winfield, Benzimidazoles diminish ERE transcriptional activity and cell growth in breast cancer cells, Biochem. Biophys. Res. Commun. 450 (2014) 1358–1362.
[11] C.P. Miller, M.D. Collini, B.D. Tran, H.A. Harris, Y.P. Kharode, J.T. Marzolf, R.A. Moran, R.A. Henderson, R.H.W. Bender, R.J. Unwalla, L.M. Greenberger, J.P. Yardley, M.A. Abou-Gharbia, C.R. Lyttle, B.S. Komm, Design, synthesis, and preclinical characterization of novel, highly selective indole estrogens, J. Med. Chem. 44 (2001) 1654–1657.
[12] R. Jeselsohn, in: A Study of Palbociclib in Combination with Bazedoxifene in Hormone Receptor Positive Breast Cancer, ClinicalTrials.gov, Dana-Farber Cancer Institute, 2017 as downloaded on January 22, 2017 from, https://clinicaltrials.gov/ct2/show/record/NCT02448771.
[13] R. Lindsay, J.C. Gallagher, R. Kagan, J.H. Pickar, G. Constantine, Efficacy of tissue-selective estrogen complex of bazedoxifene/conjugated estrogens for osteoporosis prevention in at-risk postmenopausal women, Fertil. Steril. 92 (2009) 1045–1052.
[14] V.K. Gupta, Y. Bhalla, V. Jaitak, Impact of ABC transporters, glutathione conjugates in MDR and their modulation by flavonoids: an overview, Med. Chem. Res. 23 (2014) 1–15.
[15] B. Meunier, Hybrid molecules with a dual mode of action: dream or reality? Acc. Chem. Res. 41 (2008) 69–77.
[16] Y.C. Mayur, G.J. Peters, V.V.S. Rajendra Prasad, C. Lemos, N.K. Sathish, Design of new drug molecules to be used in reversing multidrug resistance in cancer cells, Curr. Cancer Drug Targets 9 (2009) 298–306.
[17] V.R. Solomon, C. Hu, H. Lee, Hybrid pharmacophore design and synthesis of isatin-benzothiazole analogs for their anti-breast cancer activity, Bioorg. Med. Chem. 17 (2009) 7585–7592.
[18] M. Fares, W.M. Eldehna, S.M. Abou-Seri, H.A. Abdel-Aziz, M.H. Aly, M.F. Tolba, Design, synthesis and in vitro antiproliferative activity of novel isatin-quinazoline hybrids, Arch. Pharmazie 348 (2015) 144–154.
[19] J. Sidhu, R. Singla, E. Mayank, V. Jaitak, Indole derivatives as anticancer agents for breast cancer therapy: a review, Anti Canc. Agents Med. Chem. 16 (2015)

160–173.
[20] T.T.Y. Wang, M.J. Milner, J.A. Milner, Y.S. Kim, Estrogen receptor α as a target for indole-3-carbinol, J. Nutr. Biochem. 17 (2006) 659–664.
[21] L.M. Greenberger, T. Annable, K.I. Collins, B.S. Komm, C.R. Lyttle, C.P. Miller, P.G. Satyaswaroop, Y. Zhang, P. Frost, A new antiestrogen, 2-(4-hydroxyphenyl)-3-methyl-1-[4-(2-piperidin-1-yl-ethoxy)-benzyl]-1H-indol-5-ol hydrochloride (ERA-923), inhibits the growth of tamoxifen-sensitive and-resistant tumors and is devoid of uterotropic effects in mice and rats, Clin. Canc. Res. 7 (2001) 3166–3177.
[22] K. Shah, S. Chhabra, S.K. Shrivastava, P. Mishra, Benzimidazole: a promising pharmacophore, Med. Chem. Res. 22 (2013) 5077–5104.
[23] Y. Bansal, O. Silakari, The therapeutic journey of benzimidazoles: a review, Bioorg. Med. Chem. 20 (2012) 6208–6236.
[24] S. Caron, B.P. Jones, L. Wei, Preparation of substituted benzimidazoles and imidazopyridines using 2,2,2-trichloroethyl imidates, Synth 44 (2012) 3049–3054.
[25] H.M. Weir, R.H. Bradbury, M. Lawson, A.A. Rabow, D. Buttar, R.J. Callis, J.O. Curwen, C. de Almeida, P. Ballard, M. Hulse, AZD9496: an oral estrogen receptor inhibitor that blocks the growth of ER-positive and ESR1-mutant breast tumors in preclinical models, Canc. Res. 76 (2016) 3307–3318.
[26] W.O. Foye, Foye's Principles of Medicinal Chemistry, Lippincott Williams & Wilkins, 2008.
[27] X. Fan, J. Qin, Benzimidazole-2-piperazine Heterocyclic Compound as PARP Inhibitor Useful in Treatment of Various Diseases and its Preparation CN104230896A, 2014, 42pp.
[28] X. Yang, L. Wang, C. Li, Y. Zhan, J. Liu, T. Luo, H. Yan, S. Zhang, W. Li, X. Wen, T. Peng, L. Li, Substance as Tyrosine Kinase Inhibitor and its Preparation WO2014201587A1, 2014, 33pp.
[29] M. Al-Bader, C. Ford, B. Al-Ayadhy, I. Francis, Analysis of estrogen receptor isoforms and variants in breast cancer cell lines, Exp. Ther. Med. 2 (2011) 537–544.
[30] A. Strom, J. Hartman, J.S. Foster, S. Kietz, J. Wimalasena, J.A. Gustafsson, Estrogen receptor beta inhibits 17beta-estradiol-stimulated proliferation of the breast cancer cell line T47D, Proc. Natl. Acad. Sci. U. S. A 101 (2004) 1566–1571.
[31] Y.Q. Fang, Y.Z. Weng, W.Q. Huang, L. Sun, Localization of the estrogen receptor alpha and beta-subtype in the nervous system, Hatschek's pit and gonads of amphioxus, Branchiostoma belcheri, Shi Yan Sheng Wu Xue Bao 36 (2003) 368–374.
[32] J. Kurebayashi, T. Otsuki, H. Kunisue, K. Tanaka, S. Yamamoto, H. Sonoo, Expression levels of estrogen receptor-α, estrogen receptor-β, coactivators, and corepressors in breast cancer, Clin. Canc. Res. 6 (2000) 512–518.
[33] R. Singla, V. Jaitak, Multitargeted molecular docking study of natural-derived alkaloids on breast cancer pathway components, Curr. Comput. Aided Drug Des. 13 (2017). E-pub Ahead of Print.
[34] M. Dhiman, M.P. Zago, S. Nunez, A. Amoroso, H. Rementeria, P. Dousset, F.N. Burgos, N.J. Garg, Cardiac-oxidized antigens are targets of immune recognition by antibodies and potential molecular determinants in chagas disease pathogenesis, PLoS One 7 (2012), e28449.
[35] A.K. Mantha, M. Dhiman, G. Taglialatela, R.J. Perez-Polo, S. Mitra, Proteomic study of amyloid beta (25–35) peptide exposure to neuronal cells: impact on APE1/Ref-1's protein–protein interaction, J. Neur. Res. 90 (2012) 1230–1239.
[36] N.J. Kruger, The Bradford method for protein quantitation, in: J.M. Walker (Ed.), The Protein Protocols Handbook, Humana Press, Totowa, NJ, 2009, pp. 17–24.